



HAL
open science

Cool Flame of Methylcyclohexene Isomers in a Jet-Stirred Reactor: Orbitrap Characterization of Highly Oxidized Products

Zahraa Dbouk, Bakr Hoblos, Roland Benoit, Nesrine Belhadj, Philippe Dagaut

► **To cite this version:**

Zahraa Dbouk, Bakr Hoblos, Roland Benoit, Nesrine Belhadj, Philippe Dagaut. Cool Flame of Methylcyclohexene Isomers in a Jet-Stirred Reactor: Orbitrap Characterization of Highly Oxidized Products. *Energy & Fuels*, 2024, 38 (21), pp.20777-20790. 10.1021/acs.energyfuels.4c03753 . hal-04729551

HAL Id: hal-04729551

<https://hal.science/hal-04729551v1>

Submitted on 10 Oct 2024

HAL is a multi-disciplinary open access archive for the deposit and dissemination of scientific research documents, whether they are published or not. The documents may come from teaching and research institutions in France or abroad, or from public or private research centers.

L'archive ouverte pluridisciplinaire **HAL**, est destinée au dépôt et à la diffusion de documents scientifiques de niveau recherche, publiés ou non, émanant des établissements d'enseignement et de recherche français ou étrangers, des laboratoires publics ou privés.

Copyright

Cool Flame of Methylcyclohexene Isomers in a Jet-Stirred Reactor: Orbitrap Characterization of Highly Oxidized Products.

Zahraa Dbouk^{1,2}, Bakr Hoblos^{1,2}, Roland Benoit¹, Nesrine Belhadj^{1,2}, Philippe Dagaut^{1,*}

¹ CNRS, ICARE, 1C Avenue de la recherche scientifique, 45071 cedex 2, Orléans, France

² Université d'Orléans, Avenue du Parc Floral, 45067 Orléans, France

ABSTRACT: Terpenes which could be used as biofuels have relatively complex chemical structures and oxidation pathways. Therefore, studying the oxidation of simpler model-fuels, such as substituted cyclohexene isomers, could be useful. In this work, the oxidation of three isomers of methylcyclohexene (MCHX) was performed in a jet-stirred reactor over a temperature range of 500 to 1150 K under fuel-lean conditions (equivalence ratio $\varphi = 0.5$), with a residence time of 2 seconds and a pressure of 10 bar. The mole fractions of the MCHX isomers were measured using gas chromatography and flame ionization detection (GC-FID). A relatively strong cool flame was observed under the present experimental conditions (60-70 % fuel conversion), allowing the specific low-temperature oxidation products to be analyzed qualitatively using Orbitrap Q-Exactive high-resolution mass spectrometry. This was done after direct injection, or chromatographic separation via reversed-phase ultra-high-performance liquid chromatography (RP-UHPLC), and soft ionization using atmospheric pressure chemical ionization in both positive and negative modes. H/D exchange using deuterated water (D₂O) was performed to assess the presence of OH or OOH groups in the products. The reaction of 2,4-dinitrophenylhydrazine (2,4-DNPH) with oxidation samples was used to assess the presence of C=O containing compounds. A large number of oxidation products, including highly oxygenated organic molecules (HOMs) with more than five oxygen atoms, were observed. Unexpectedly, numerous products containing carboxylic acid and carbonyl functional groups, as well as aromatic compounds, were detected. According to this study, the MCHX isomers oxidize in a very similar manner, sharing many common oxidation products and species pertaining to the same chemical classes. Routes for the formation of oxidation products were proposed to rationalize the results.

Keywords: Jet-stirred reactor, Cool flame, Orbitrap, HOMs, Methylcyclohexene

NOMENCLATURE

APCI Atmospheric pressure chemical ionization

FIA Flow injection analysis

HCD Higher-energy collision dissociation

HESI Heated electrospray ionization

HPLC High-pressure liquid chromatography

HRMS High-resolution mass spectrometry

MS Mass spectrometry

RP-UHPLC Reverse-phase ultra-high-performance liquid chromatography

1. INTRODUCTION

Terpenes are secondary metabolites synthesized primarily by plants, but also by a limited number of insects, microorganisms, and marine fungi¹. They can be extracted using various methods such as solvent extraction and steam distillation, which are well-established and suitable for large-scale applications²⁻⁵. Terpenes have various uses and are employed as ingredients in the production of cosmetic, pharmaceutical, and food products⁶⁻¹¹. Moreover, due to their high octane number and characteristics similar to those of fuels used in internal combustion engines, such as viscosity, flash points, high energy densities, and high volumetric net heat of combustion (NHOC)¹², terpenes have the potential to serve as precursors for advanced biofuels¹³⁻¹⁹, including additives or alternatives to diesel^{13, 20}. Limonene has been tested as antiknock additive in a research piston engine²¹, showing a research octane number of 88. Additionally, their cyclic or linear structures can feature methyl branches and double bonds (Figure 1), significantly lowering melting and freezing points. Consequently, terpenes can be used as alternatives or additives for existing aviation biofuels, such as Jet-A, JP-5, and JP-8, as well as for military aircraft fuels like JP-10^{14, 22-25}. Table S1 in the supporting information presents the characteristics of these fuels and includes information on one of the most abundant terpenes, limonene. Despite their potential, the complex structure of cyclic terpenes complicates the understanding of their oxidation mechanisms, which have not been extensively studied, particularly under cool flame conditions²⁶⁻²⁷.

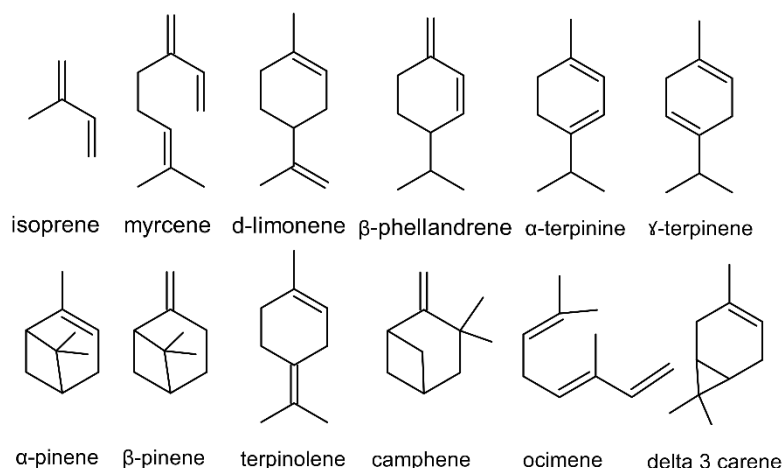
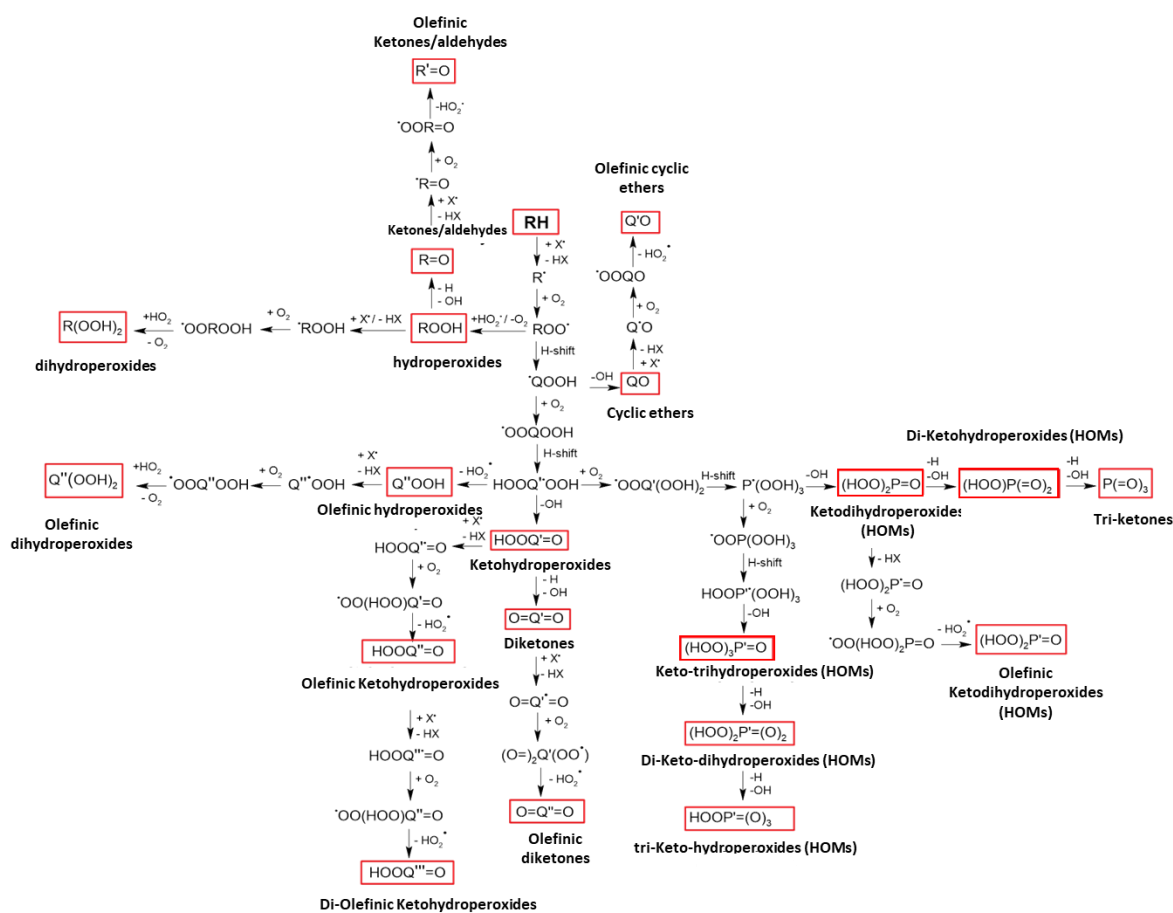


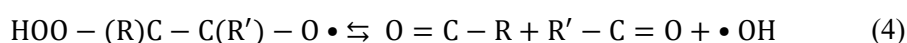
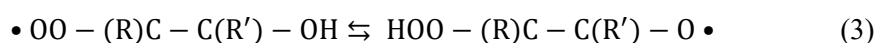
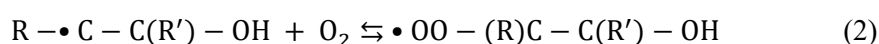
Figure 1. Chemical structures of terpenes.



Scheme 1. Reaction pathways and formation of low-temperature oxidation intermediates.

Under these conditions, hydrocarbons (RH) can react with O_2 molecules to produce oxygenated intermediates, as well as highly oxygenated compounds when three or more O_2 molecules are added to the fuel radicals, as illustrated in Scheme 1. Additional reaction pathways can occur under these conditions, such as the Korcek mechanism, which converts γ -ketohydroperoxides into carbonyl products and carboxylic acids. Evidence for the occurrence of this mechanism has recently been presented and

has been integrated into the latest combustion models²⁸⁻²⁹. Consequently, it has often been used to explain the formation of carboxylic acids during the oxidation of hydrocarbons at low temperatures^{26, 28, 30-33}. On the other hand, if the initial reactant has a carbon-carbon double bond, as in methylcyclohexenes, the Waddington mechanism may take place³⁴. This mechanism involves the addition of an OH group to the C=C double bond (1), followed by the addition of O₂ (2), a hydrogen-shift from the -OH group to the -OO• peroxy group leading to decomposition (3). Consequently, the hydroxyl radical initially consumed is ultimately regenerated at the end of this reaction process (4).

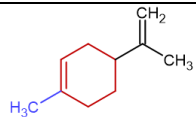
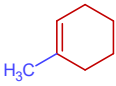
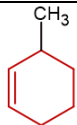
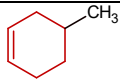


In tropospheric chemistry, researchers are focused on the oxidation of alkylcycloalkenes with simplified structures. This approach aims to enhance the understanding of the reaction mechanisms involved in the gas-phase ozonolysis of complex cycloalkenes, particularly major monoterpenes such as limonene and α -pinene. For example, Berndt et al.³⁵ studied the gas-phase ozonolysis of C5-C8 cycloalkenes as well as the subsequent reactions of highly oxidized RO₂ radicals formed with NO, NO₂, SO₂, and other RO₂ radicals, in order to understand the oxidation mechanisms of more complex alkenes. Similarly, Rissanen et al.³⁶ studied the formation of highly oxidized products during the ozonolysis of endocyclic alkenes, specifically 1-methylcyclohexene and 4-methylcyclohexene, in borosilicate glass tubular reactors at room temperature ($T = 293 \pm 3$ K) and atmospheric pressure. The oxidation products formed were analyzed using a time-of-flight mass spectrometer with atmospheric pressure interface and chemical ionization. This study aimed to compare the oxidation mechanisms of endocyclic alkenes with those of α -pinene and to deepen the understanding of these processes. In the same way, Hatakeyama et al.³⁷ conducted experiments to study the reactions of ozone with 1-methylcyclohexene and methylene cyclohexane in air, thereby simulating tropospheric conditions. The yields of gaseous products from 1-methylcyclohexene were compared with α -pinene, while yields from methylene cyclohexane were compared with β -pinene, to determine the similarity of the reaction mechanisms. The results confirmed that the reactions of ozone with α -pinene can follow a similar mechanism to that observed during the oxidation of 1-methylcyclohexene and methylene cyclohexane. Furthermore, other ozonolysis studies of alkylcycloalkenes have been performed to understand how the structure of a hydrocarbon precursor influences the formation of oxidation products and to predict the potential formation for compounds lacking yield data, particularly for tropospheric relevant precursors such as biogenic monoterpenes and sesquiterpenes³⁸⁻³⁹. These studies motivated us to investigate the oxidation of simpler model compounds under cool flame conditions, to better understand the kinetic oxidation mechanisms of complex

endocyclic compounds. Furthermore, methylcyclohexenes are formed during the oxidation of components of aviation surrogate fuels such as methylcyclohexane⁴⁰⁻⁴¹, which increase the importance of studying their oxidation. However, they were not selected to be terpenes model-fuel or surrogate. The main goal of this work is to describe the oxidation of methylcyclohexene isomers under cool-flame conditions.

This work aims to investigate the oxidation mechanisms of three isomers of methylcyclohexene (MCHX): 1-methyl-1-cyclohexene (1M1CHX), 3-methyl-1-cyclohexene (3M1CHX), and 4-methyl-1-cyclohexene (4M1CHX) under cool flame conditions. We conducted oxidation experiments in a jet-stirred reactor (JSR), and the resulting products were analyzed using high-resolution mass spectrometry (Orbitrap Q-Exactive HRMS). Whereas combustion in engines occurs at higher pressures, we operated at 10 bar since mostly the relative importance of reaction pathways are affected by pressure⁴²⁻⁴³. Oxidation products were either separated by ultra-high-performance liquid chromatography (UHPLC) before HRMS analysis or analyzed directly through flow-injection analysis (FIA). The characterization of oxidation products dissolved in acetonitrile (ACN) was performed using 2,4-dinitrophenylhydrazine (2,4-DNPH) derivatization of carbonyls and hydrogen/deuterium (H/D) exchange. Experimental data from the oxidation of the three isomers were compared to evaluate their kinetic similarities and to assess whether structural differences impact the reaction mechanisms and pathways. This study aims to provide insights into the diverse reaction mechanisms involved in the oxidation of complex cyclic alkenes at low temperatures. This is particularly relevant for understanding the oxidation of monoterpenes such as limonene and α -pinene, which exhibit structural similarities to MCHX, as highlighted in Table 1.

Table 1. Structures of cyclic alkenes: limonene, α -pinene, 1M1CHX, 3M1CHX, and 4M1CHX, showing their structural similarities.

Monoterpenes (C ₁₀ H ₁₆)	Limonene CAS 138-86-3	
	α -Pinene CAS 80-56-8	
MCHX isomers (C ₇ H ₁₂)	1M1CHX CAS 591-49-1	
	3M1CHX CAS 591-48-0	
	4M1CHX CAS 591-47-9	

2. EXPERIMENTAL

2.1 Oxidation experiments. Oxidation experiments were carried out in a fused silica JSR (42 mL), described earlier⁴⁴⁻⁴⁵. The initially liquid fuels (1-methyl-1-cyclohexene, >98% pure, from TCI; 3-methyl-1-cyclohexene >93% pure, from TCI; 4-methyl-1-cyclohexene >98% pure, from TCI) were pumped by an HPLC pump (LC10 AD VP Shimadzu[®]) into a vaporizer assembly fed with an auxiliary nitrogen (N₂) flow (50 L/h), used to atomize the fuel prior to its vaporization⁴⁶⁻⁴⁷. The fuel, pushed by that flow of nitrogen, is atomized through an annular hole. The resulting spray enters a vaporizer maintained at 120 °C, a temperature slightly higher than the fuel boiling point. The primary flow of N₂ (diluent, 99.99 pure) was brought to the reactor in the same stream with the oxygen (O₂, 99.995% pure) flow. To avoid premature oxidation, MCHX isomer–N₂ and oxygen–N₂ were introduced separately into the JSR. The flow rates of nitrogen and oxygen were controlled using mass flow meters, which ensured accurate regulation of the experimental conditions. Additionally, a thermocouple protected by a thin-wall fused silica housing (0.1 mm Pt-Pt/Rh-10% wires) was moved along the vertical axis of the JSR to verify thermal homogeneity (gradient < 2 K/ cm). The oxidation of the fuels was conducted over the temperature range 500–1150 K, and at 10 bar. The three isomers were oxidized under identical conditions. We used 3000 ppm of each hydrocarbon under fuel-lean conditions ($\phi = 0.5$), with a mean residence time of 2 s. Oxidation products were collected in two ways. Firstly, they were stored in Pyrex bulbs for off-line gas chromatography analyses. Secondly, the gas mixture obtained from the fuel oxidation at 620 and 680 K was bubbled through approximately 20 mL of cold acetonitrile (273 K) for 60 minutes. The resulting samples were then stored at -15 °C for further LC-HRMS analyses. Table 2 presents the experimental conditions.

Table 2. Oxidation conditions.

Initial fuel mole fraction	3000 ppm
Pressure	10 bar
Equivalence ratio (ϕ)	0.5
Residence time (τ)	2 s
Oxidation temperature	500-1150 K

2.2 Chemical Analyses. Besides quantitative analyses by gas chromatography-flame ionization detection (GC-FID), oxidation products were qualitatively analyzed using high-resolution mass spectrometry (Orbitrap Q-exactive[®]). The Orbitrap Q-exactive[®] was calibrated in both positive and negative ionization modes using HESI Pierce calibration mixtures. Samples obtained at 620 and 680 K

were either directly analyzed via flow injection analysis HRMS or separated prior to analysis using reverse-phase HPLC with a C18 column (1.6 μm , 100 \AA , 100 \times 2.1 mm, Phenomenex Luna), placed in a temperature-controlled oven maintained at 40 $^{\circ}\text{C}$. For HPLC separation, 3 μL of samples were eluted with a water-acetonitrile (ACN) mixture at a flow rate of 300 $\mu\text{L}/\text{min}$, using a gradient from 5% to 90% ACN over 45 minutes. An atmospheric pressure chemical ionization (APCI) source was used to ionize the oxidation products in both positive and negative modes. For FIA-APCI-HRMS analyses, the APCI settings were as follows: vaporizer temperature of 120 $^{\circ}\text{C}$, capillary transfer temperature of 200 $^{\circ}\text{C}$, sheath gas flow of 4 a.u., auxiliary gas flow of 0 a.u., sweep gas flow of 0 a.u., and corona discharge current of 5.4 μA . For HPLC-APCI-HRMS analyses, the sheath gas flow was set to 50 a.u., the auxiliary gas flow to 5 a.u., and the corona discharge current to 5 μA . All other parameters remained the same as in the FIA-APCI-HRMS analyses. To obtain structural information about oxidation intermediates, RP-UHPLC-MS/MS analyses were performed with a collision cell energy of 10 eV. Additionally, similar to what was done in previous studies^{26,48}, the presence of carbonyl compounds was assessed by adding 2,4-DNPH to our oxidation samples. 300 μL of a 2,4-DNPH solution was introduced into 1 mL of the samples after acidifying the mixture by adding 30 μL of H_3PO_4 (0.1 M). We let the reaction proceed for up to 8 h before performing the analysis. The presence of hydroxyl ($-\text{OH}$) and hydroperoxyl ($-\text{OOH}$) groups in the oxidation products was examined using H/D exchange by adding 300 μL of D_2O to 1 mL of samples (reaction time of 20-30 min).

3. RESULTS AND DISCUSSION

As previously mentioned, 3000 ppm of each MCHX isomer were oxidized at temperatures ranging from 500 to 1150 K, a pressure of 10 bar, a constant residence time of 2 s and in the presence of an excess of O_2 ($\phi = 0.5$). As shown in Figure 2, the conversion of fuels was relatively high (~ 60 -70 %) under these cool-flame conditions and the production of specific cool-flame products was observable.

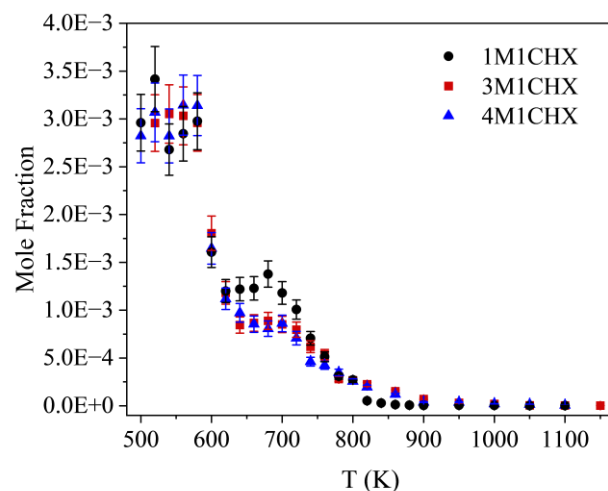


Figure 2. Mole fractions of the fuels measured by GC-FID. The analyses were performed using a 50 m capillary Al₂O₃-KCl column with an He flow of 1.5 mL/min (T₀=70 °C, gradient = 10 °C/min to T_f=200 °C).

3.1 Products of Initial O₂ Addition. In the oxidation samples of the three isomers (1M1CHX, 3M1CHX, and 4M1CHX), we detected the products resulting from the initial O₂ addition to the fuel radicals. These products included hydroperoxides, and carbonyl compounds or cyclic ethers formed according to the mechanism presented in Scheme 1.

Hydroperoxides were identified using H/D exchange with D₂O (see Section 2.2). Following this exchange, a clear signal corresponding to C₇H₁₁D₁O₂ (C₇H₁₂D₁O₂⁺, *m/z* 130.0972, C₇H₁₀D₁O₂⁻, *m/z* 128.0827) was detected in the oxidation sample of each MCHX isomer, confirming the presence of these compounds. During the oxidation of MCHX isomers, we observed the formation of nearly identical C₇H₁₂O₂ isomers, although their quantities varied, as shown in Figure 3. The differentiation between hydroperoxides and other isomers containing at least one C=O group was achieved by adding 2,4-DNPH (e.g., Figure S1, Supporting Information). The black lines represent the signals of the isomers before their reaction with DNPH, while the red lines represent their signals after the reaction with DNPH. When an isomer reacts with DNPH, a portion of it is consumed to form a stable dinitrophenylhydrazone, leading to a reduction in its signal intensity. However, we have observed that for isomers lacking a carbonyl group, their signal intensity sometimes increases after adding DNPH. The exact reason for this increase is unclear, but it may be related to the pH of the medium. The reaction with DNPH occurs in an acidic environment, which can influence the chemical ionization of isomers in APCI. In such conditions, the ionization efficiency of these compounds might be affected due to changes in their protonation or deprotonation equilibria. The signal intensity of the isomers primarily depends on their concentration and secondarily on their ability to be ionized in the ionization source.

Unfortunately, the structural characterization of these isomers was not feasible from the MS/MS spectrum. They could potentially be carbonyl products formed through ring-opening mechanisms. Notably, if 1M1CHX, 3M1CHX, and 4M1CHX reacted according to the Waddington mechanism, we would expect to observe specific carbonyl products: 6-oxo-heptanal, 2-methyl-6-oxo-hexanal, and 3-methyl-6-oxo-hexanal, respectively. However, 6-oxo-heptanal was found only in trace amounts in the 1M1CHX oxidation sample identified using a standard (Figure S2, Supporting Information). We compared the MS/MS spectra of a 6-oxo-heptanal standard with that of the isomer eluted at around 7 minutes. Identical spectra with matching fragments were observed, confirming the presence of 6-oxo-heptanal. These spectra are included in the supporting information (Figure S2b). This suggests that the Waddington mechanism is not very favorable during 1M1CHX oxidation under our conditions, or that the formed quantities of 6-oxo-heptanal were consumed to form other oxidation intermediates. Scheme 2 presents the formation mechanism of 6-oxo-heptanal via the Waddington mechanism. In contrast,

Waddington products were not found in the 3M1CHX and 4M1CHX oxidation samples, indicating that these isomers do not follow the Waddington mechanism, unlike their isomer 1M1CHX.

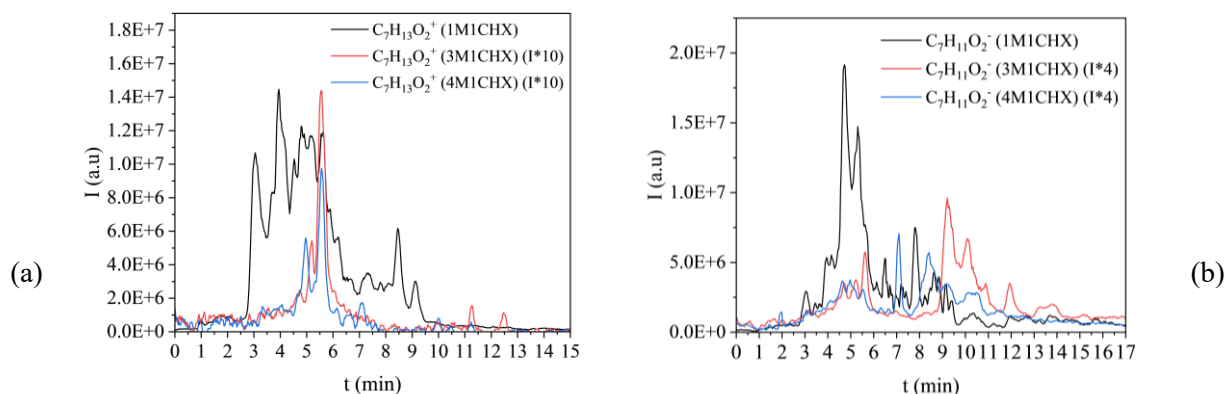
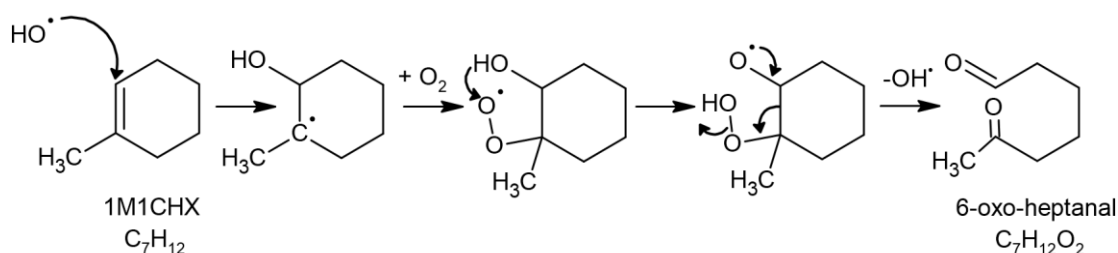


Figure 3. Chromatograms of $C_7H_{12}O_2$ isomers ionized with (a) APCI (+) ($C_7H_{13}O_2^+$, m/z 129.0910) and (b) APCI (-) ($C_7H_{11}O_2^-$, m/z 127.0764). The sample was taken at 680 K. The black chromatogram represents isomers formed during the oxidation of 1M1CHX, while the red and blue chromatograms correspond to isomers formed during the oxidation of 3M1CHX and 4M1CHX, respectively.



Scheme 2. Oxidation of the endocyclic double bond of 1M1CHX via the Waddington mechanism.

The dehydration of hydroperoxides ($C_7H_{12}O_2$) leads to the formation of carbonyl compounds ($C_7H_{10}O$), as shown in Scheme 1 (Introduction). As for the $C_7H_{12}O_2$ isomers, the three fuels share common $C_7H_{10}O$ isomers (see Figure 4), but not all these isomers are shared. Likewise, carbonyl products were distinguished from cyclic ethers by 2,4-DNPH derivatization, as illustrated in Figure S3, in the supporting information. Isomers eluted at retention times (Rt) = 6.9, 7.9, 8.2, and 10.64 min correspond to carbonyl compounds, while those eluted between 11.5 and 12.9 min correspond either to cyclic ethers or to olefinic alcohols. A signal corresponding to $C_7H_9D_1O$ ($C_7H_{10}D_1O^+$, m/z 112.0867), indicating the presence of olefinic alcohols, was detected in the samples. We noticed that during the oxidation of MCHX isomers, the formation of carbonyl groups predominates over that of other functional isomers. The MS/MS spectra of all $C_7H_{10}O$ isomers show the same fragment, though with different intensities, making structural characterization through MS/MS spectra challenging. However, the isomer eluted at 6.9 minutes was identified as 3-methyl-2-cyclohexen-1-one using a standard.

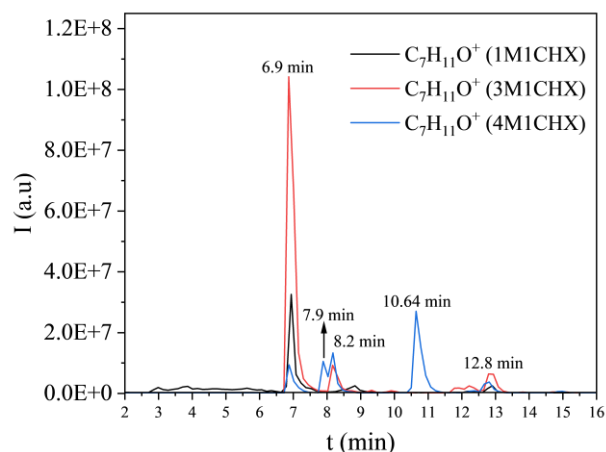


Figure 4. Chromatograms of $C_7H_{10}O$ isomers ionized with APCI (+) ($C_7H_{11}O^+$, m/z 111.0806), formed in the JSR during MCHX oxidation at 680 K. The black chromatogram represents isomers formed during the oxidation of 1M1CHX, while the red and blue chromatograms correspond to isomers formed during the oxidation of 3M1CHX and 4M1CHX, respectively.

3.2 Aromatics and non-Oxygenated Products. Additionally, we identified other oxidation products, such as aromatic compounds, including cresols. Figure 5 displays the chromatograms of these aromatic isomers detected during the oxidation of the MCHX isomers. Para-cresol and ortho-cresol were identified using their standards, eluting at $R_t = 11.05$ min and $R_t = 11.65$ min, respectively. On the other hand, meta-cresol, was identified through MS/MS analyses. One should note that the literature lacks detailed references on the fragmentation mechanisms of molecules similar to our oxidation products. Therefore, to enhance our understanding of these mechanisms, we analyzed the MS/MS spectra of several standards, including aromatic products. Interestingly, we observed that these aromatic compounds did not fragment at 10 eV in the HCD (Higher-energy Collisional Dissociation) cell. Although we did not have the standard for meta-cresol, we assigned it to the minor isomer eluted at $R_t = 9.8$ min, which did not fragment in the HCD.

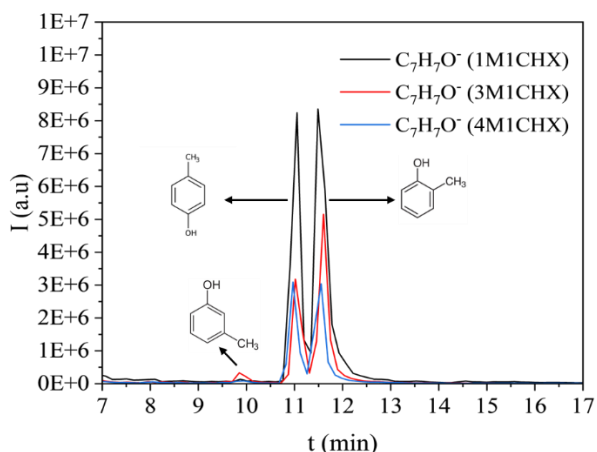


Figure 5. Chromatograms of C_7H_8O isomers ionized with APCI ($-$) ($C_7H_7O^-$, m/z 107.0502), formed in the JSR during MCHX oxidation at 680 K. The black chromatogram represents isomers formed during the oxidation of 1M1CHX, while the red and blue chromatograms correspond to isomers formed during the oxidation of 3M1CHX and 4M1CHX, respectively.

Regarding the formation mechanism of cresols, several hypotheses can be proposed. One possibility is that cresols are formed from the oxidation of hydroxymethylcyclohexene ($C_7H_{10}O$), followed by HO_2 elimination. Cresols were also identified by Herbinet et al.⁴⁹ among the products of toluene oxidation in a Jet-Stirred Reactor (JSR) over a temperature range of 500 to 1100 K. Similarly, Schwantes et al.⁵⁰ observed the formation of cresols from toluene during its oxidation in the presence of hydroxyl radicals (OH) and nitric oxide (NO) in a Teflon chamber at 309 K. Therefore, it is possible that the cresol isomers detected in this study were originated from the oxidation of toluene, which was also found among the oxidation products of the three isomers. The chromatogram of cresols shown in Figure 5 was obtained from the analysis of sample resulting from the oxidation of MCHX isomers at 680 K. Under the same experimental conditions, toluene mole fractions were measured by GC-FID. We found values of 1.04×10^{-4} , 1.06×10^{-4} , and 9.79×10^{-5} for 1M1CHX, 3M1CHX, and 4M1CHX, respectively. Cresols mole fractions were not measured but analyzed qualitatively using HRMS. Nevertheless, one can see from Fig. 5 that there is not clear correlation between the toluene mole fractions (nearly equal) obtained for the three fuels and the variable signal intensities recorded for cresols. Due to the presence of multiple reaction pathways (Scheme 3), establishing a direct quantitative correlation between the amount of toluene and the observed levels of cresols remains challenging. The variability in reaction mechanisms means we lack detailed information on which mechanisms are occurring and their relative importance for each fuel. Given these complexities, directly linking toluene concentrations to cresol formation may not be feasible at this stage. Besides toluene, other non-oxygenated products were also detected, such as the diene isomers (C_7H_{10}) (Figure S4, Supporting Information). These can result from HO_2 elimination following the initial O_2 addition to the fuel radicals (reactions 5, 6, and 7). Additionally, the oxidation of these dienes can lead to the formation of cresols. Scheme 3 illustrates the various mechanisms that could produce cresol isomers.



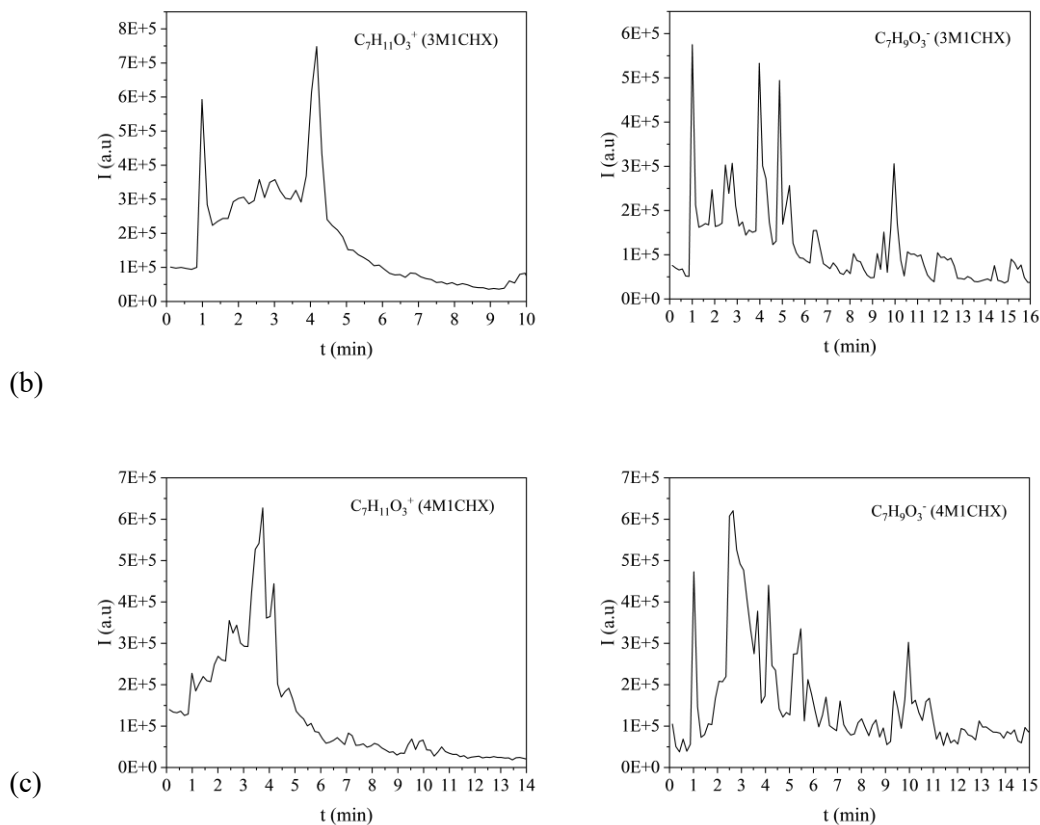


Figure 6. Chromatograms of $C_7H_{10}O_3$ isomers formed in the JSR during the oxidation of 1M1CHX (a), 3M1CHX (b), and 4M1CHX (c) at 680 K. Chromatograms on the left are for isomers ionized with APCI (+) ($C_7H_{11}O_3^+$, m/z 143.0699), while those on the right are for isomers ionized with APCI (-) ($C_7H_9O_3^-$, m/z 141.0546).

3.3.1 1M1CHX Oxidation Products. All the $C_7H_{10}O_3$ isomers shown in the Figure 6 (a), formed during 1M1CHX oxidation, react with 2,4-DNPH; they contain at least one C=O group. Furthermore, the observation of a first H/D exchange ($C_7H_{10}D_1O_3^+$ ion, m/z 144.0765) with a significant intensity equivalent to $C_7H_{11}O_3^+$ ion (m/z 143.0699), indicates the presence of OH or OOH functions. MS/MS spectrum of the detected isomers were studied in order to characterize their structure. we obtained the same fragments from the fragmentation of all isomers in the HCD cell, although their intensities vary. This suggests that the detected isomers are probably position isomers. An example of this similarity is shown in Figure S5, in the supporting information. As we have mentioned previously, to enhance our understanding of fragmentation mechanisms, we analyzed the MS/MS spectra of several standards. We noticed that at 10 eV, the fragmentation of non-branched or slightly branched cyclic molecules is not significant; the intensity of the parent ion is significantly higher than that of fragments, unlike linear species. Moreover, carboxylic acids lose CH_2O_2 in positive mode from the protonated ion $[M+H]^+$, while in negative mode, they lose CO_2 from the deprotonated ion $[M-H]^-$. This last observation was also

reported by Liang et al.⁵¹ and Demarque et al.⁵². For isomers eluted between 2 et 4.5 min, their high fragmentation rate indicates that they are probably linear isomers. On the other hand, in all their MS/MS in positive mode, a $C_6H_5O^+$ fragment (m/z 97.0651) corresponding to a CH_2O_2 loss from the parent ion $C_7H_{11}O_3^+$ (m/z 143.0699) was detected with a significant intensity. An example is shown in Figure 7 (a). Similarly, in negative mode, a fragment $C_6H_5O^-$ corresponding to the loss of CO_2 from the parent ion $C_7H_9O_3^-$ (m/z 141.0546) was observed in the MS/MS spectrum of all isomers. An example of negative MS/MS is illustrated in Figure 7 (b). These observations indicate the presence of a carboxylic acid function. Also, in the same MS/MS spectrum, several CO losses were observed (Figure 7, fragments $C_5H_9^+$ and $C_4H_7^+$), suggesting the presence of a carbonyl function, either a ketone or an aldehyde. Therefore, the detected isomers are likely carboxylic keto/aldo acids rather than KHPs.

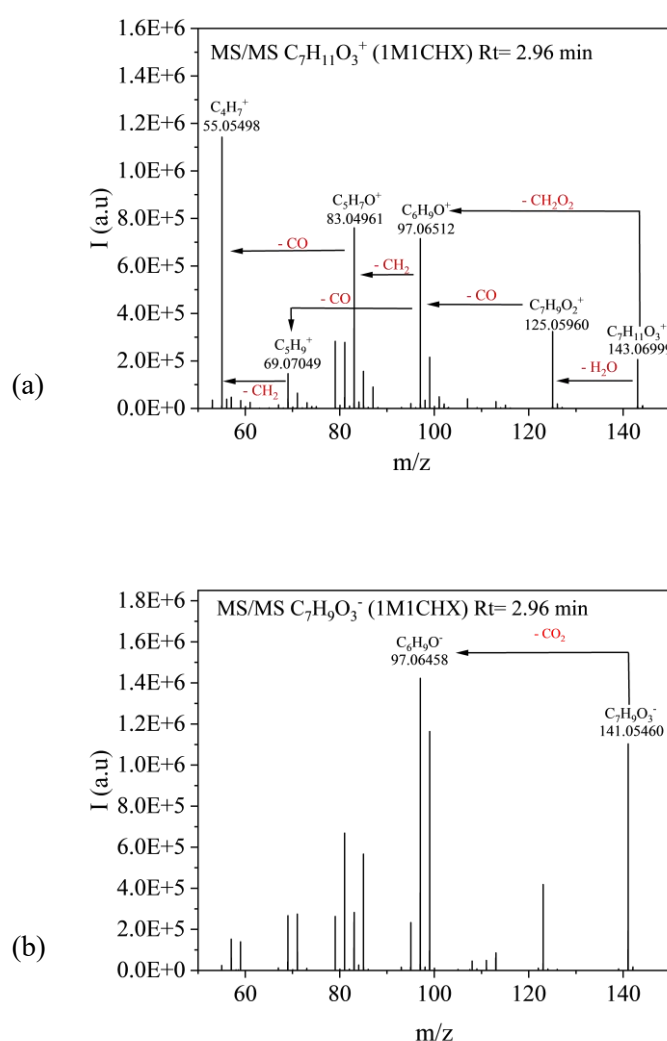
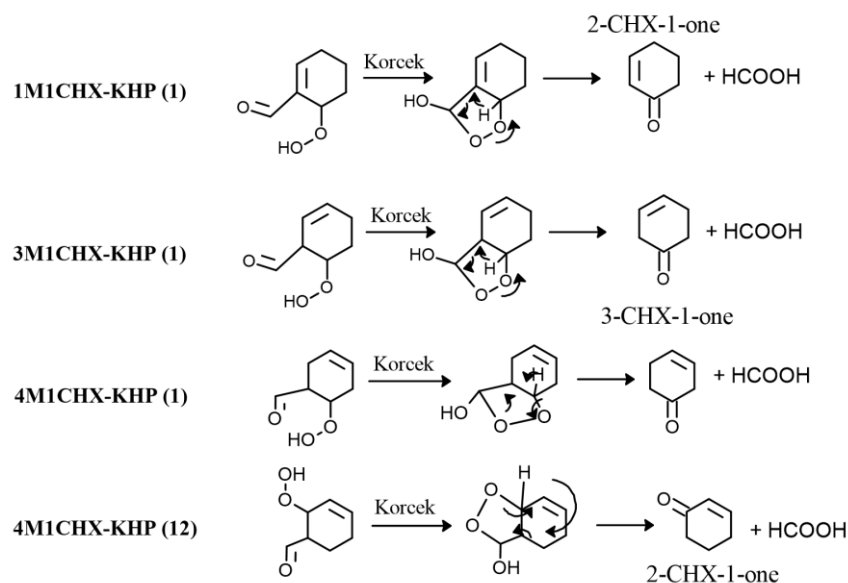


Figure 7. MS/MS of the $C_7H_{10}O_3$ isomers formed during 1M1CHX oxidation at 680 K, eluted at $R_t = 2.96$ min, and ionized with (a) APCI (+) ($C_7H_{11}O_3^+$, m/z 143.0699) and (b) APCI (-) ($C_7H_9O_3^-$, m/z 141.0546).

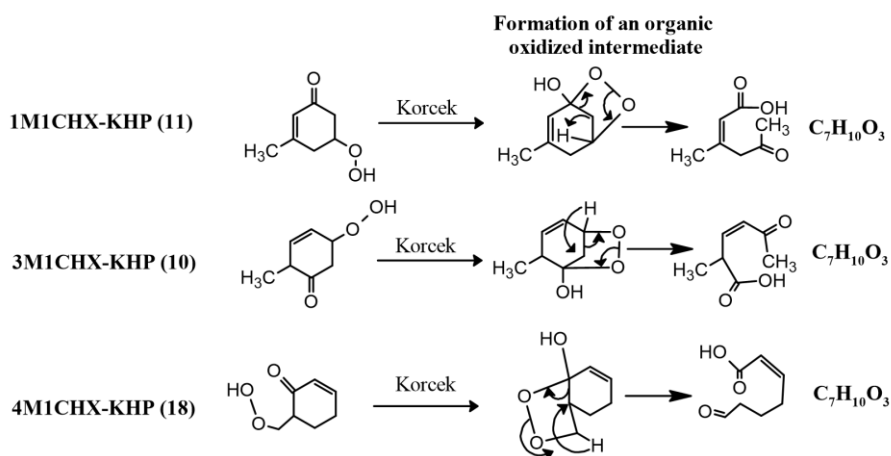
3.3.2. 3M1CHX and 4M1CHX Oxidation Products. Several $C_7H_{10}O_3$ isomers were found in the oxidation samples of 3M1CHX and 4M1CHX. After studying their MS/MS spectra, we observed that they belong to the same chemical family as the isomers detected in the 1M1CHX oxidation sample. They also exhibited similar MS/MS spectra, with fragments confirming the presence of a carboxylic group in their structure, indicated by $[M+H-CH_2O_2]^+$ and $[M-H-CO_2]^-$, as well as a carbonyl group (Figure S6, Supporting Information).

To identify common isomers, the chromatograms of $C_7H_{10}O_3$ isomers were compared. While some compounds elute at the same retention time (Figure S7, supporting information), they are not always the same isomers, as confirmed by MS/MS spectra. For instance, the MS/MS spectra of the isomer eluted at $R_t = 2.93$ min from both 1M1CHX and 3M1CHX oxidations show similar fragments but differ in their fragment ratios (Figure S8, supporting information), indicating different isomers despite shared functionalities (carboxylic acid and carbonyl group). Conversely, isomers eluted at $R_t = 4.09$ min from 3M1CHX and 4M1CHX oxidations display identical MS/MS spectra with matching fragment ratios (Fig. S8, Supporting Information), confirming they are the same isomers. Carboxylic acid formation is rarely observed in low-temperature hydrocarbon combustion experiments. Furthermore, the mechanisms describing their formation are poorly documented in the literature. One of these mechanisms is the Korcek mechanism already introduced. It leads to the formation of carboxylic acids and carbonyls by the decomposition of γ -KHPs.

Figures S9, S10, and S11 (Supporting Information) illustrate the different proposed KHP isomers that can be formed during the oxidation of 1M1CHX, 3M1CHX, and 4M1CHX, respectively. Among the isomers of 1M1CHX, six isomers (1, 7, 10, 11, 15, and 17) can decompose via the Korcek mechanism. For 3M1CHX, four isomers (1, 7, 10, and 11) can decompose, and for 4M1CHX, six isomers (1, 12, 15, 17, 18, and 23) can decompose through this mechanism. The decomposition of isomer (1) for each hydrocarbon, as well as isomer (12) of 4M1CHX, leads to the formation of a six-carbon atom carbonyl compound (C_6H_8O) and formic acid ($HCOOH$), as illustrated in Scheme 4. When the remaining cited isomers decompose, they produce $C_7H_{10}O_3$ isomers containing both an acid group and another carbonyl group. Scheme 5 illustrates an example of the decomposition according to the Korcek mechanism of one isomer from each hydrocarbon. The decomposition mechanisms for the remaining isomers of the three MCHX isomers are illustrated in Scheme S1 (Supporting Information).



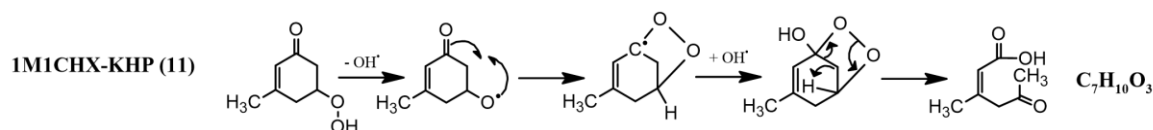
Scheme 4. Decomposition of γ -KHP isomers, potentially formed during MCHX isomers oxidation, via the Korcek mechanism, leading to cyclohexenone isomers.



Scheme 5. Decomposition of γ -KHP isomers, potentially formed during MCHX isomer oxidation, via the Korcek mechanism, leading to $C_7H_{10}O_3$ isomers.

Moreover, Goldsmith et al.⁵³ and Jalan et al.⁵⁴ reported an alternative decomposition pathway of γ -KHPs that predominantly occurs at temperatures above 600 K. It involves the unimolecular dissociation of the O-O bond of the hydroperoxyl group ($HOOP=O \rightarrow \bullet OH + OP=O$). This dissociation then leads to the formation of an oxidized organic intermediate, specifically the 5-membered ring formed during the decomposition of γ -KHPs according to the Korcek mechanism. Subsequently, this intermediate undergoes a decomposition similar to that observed in the Korcek mechanism. Therefore, the final product resulting from this decomposition is identical in both cases. Scheme 6 represents an example. Therefore, the keto/aldo-carboxylic acid isomers ($C_7H_{10}O_3$) detected in the MCHX isomers

samples could correspond to products resulting from the decomposition of γ -KHPs formed during the oxidation process.



Scheme 6. Decomposition of KHP (1), potentially formed during 1M1CHX oxidation, by unimolecular dissociation of the O-O bond of the hydroperoxyl group.

Other mechanisms described in the literature, such as those proposed by Battin-Leclerc et al.⁵⁵, Herbinet et al.⁵⁶, and Madronich et al.⁵⁷, specifically detail the formation of carboxylic acids through the oxidation of aldehyde groups. In this context, di-carbonyl $C_7H_{10}O_2$ isomers containing an aldehyde group can react to form keto/aldo-carboxylic acids ($RCHO + \bullet OH \rightarrow RC(O)OH + \bullet H$ with $R = C_6H_9O$). Although several $C_7H_{10}O_2$ isomers were detected in the oxidation samples of the three fuels, their identification was not possible. The chromatograms showing the various isomers detected in the oxidation samples of the fuels are illustrated in Figure S12 (Supporting Information).

KHPs are unstable products that, in addition to decomposing into carboxylic acids and carbonyl compounds, can undergo dehydration to form diketones, as shown in Scheme 1 ($C_7H_{10}O_3 \rightarrow C_7H_8O_2 + H_2O$). Our data confirm the presence of these diketones ($C_7H_8O_2$) in the oxidation samples of 1M1CHX, 3M1CHX, and 4M1CHX (Figure 8). We observed that MCHX isomers share nearly the same $C_7H_8O_2$ isomers. 2,4-DNPH was used to distinguish diketones from their isomers, such as di-olefinic diols, as shown in Figure S13 (Supporting Information).

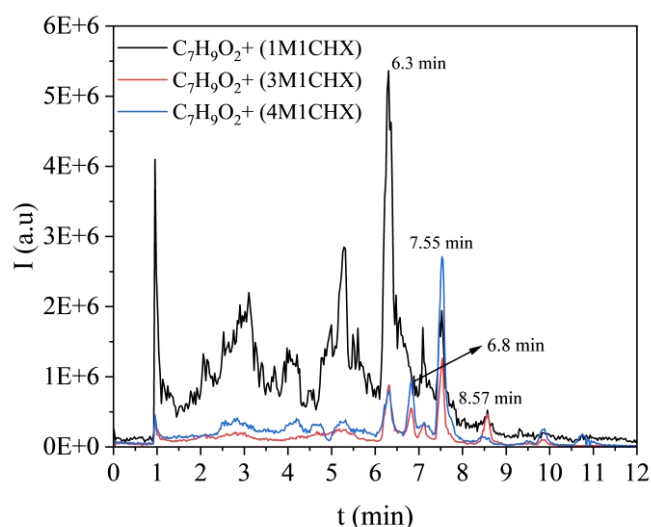


Figure 8. Chromatograms of $C_7H_8O_2$ isomers ionized with APCI (+) ($C_7H_9O_2^+$, m/z 125.0597), formed in the JSR during MCHX oxidation at 680 K. The black chromatogram represents isomers formed during

the oxidation of 1M1CHX, while the red and blue chromatograms correspond to isomers formed during the oxidation of 3M1CHX and 4M1CHX, respectively.

3.4. Other Detected Carboxylic Acids. In the oxidation samples of the MCHX fuels, we identified numerous compounds containing carboxylic acid groups. For example, besides the $C_7H_{10}O_3$ isomers, we detected $C_7H_{12}O_3$ isomers that contain a carboxylic acid function in their structures. As shown in Figure S14, 1M1CHX, 3M1CHX, and 4M1CHX share common $C_7H_{12}O_3$ isomers. However, the oxidation sample of 1M1CHX contains additional isomers formed exclusively during its oxidation. The study of common isomers MS/MS spectra allows us to identify the presence of carboxylic group function in their structure. An example of the MS/MS spectra of the isomers eluted at $R_t = 2.7$ min and $R_t = 3.17$ min is shown in the Figure 9. The presence of a fragment corresponding to the loss of CO_2 from the precursor ion ($C_6H_{11}O^-$, m/z 99.08035) confirms the existence of a carboxylic acid function. The rate of fragmentation indicates that these are linear species. However, MS/MS spectra do not provide additional information to confirm the family of the second chemical function. Since only one H/D exchange ($C_7H_{11}D_1O_3^-$, m/z 144.0776, $C_7H_{12}D_1O_3^+$, m/z 146.0922), corresponding to the OH of the carboxylic acid function, is detected in 3M1CHX and 4M1CHX oxidation samples; the second function was identified as a carbonyl group. In this case, the detected $C_7H_{12}O_3$ isomers likely correspond to keto/aldo-carboxylic acids. Among the isomers detected in the oxidation sample of 1M1CHX, a trace of 6-oxo-heptanoic acid was found after tracking it by analyzing a standard. It can be formed by the addition of OH to the endo-cyclic double bond of 1M1CHX, as illustrated in Scheme 7. Given that it was detected only in trace amounts, his oxidation pathway appears to be of minor importance under our oxidation conditions.

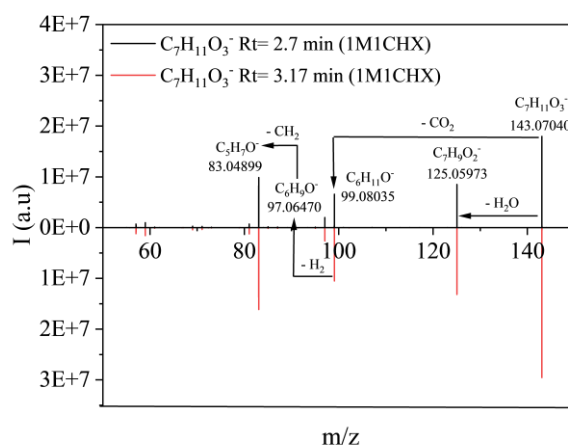
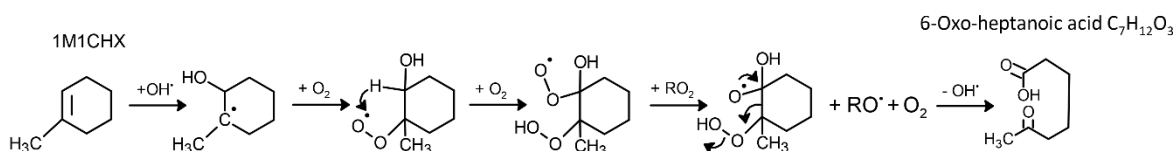
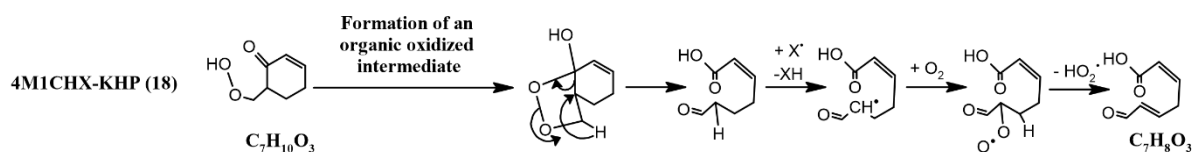


Figure 9. The MS/MS spectra of $C_7H_{12}O_3$ isomers ionized in APCI (-), formed during the oxidation of 1M1CHX in the JSR at 680 K and eluted at: $R_t = 2.7$ min (in black) and $R_t = 3.17$ min (in red).



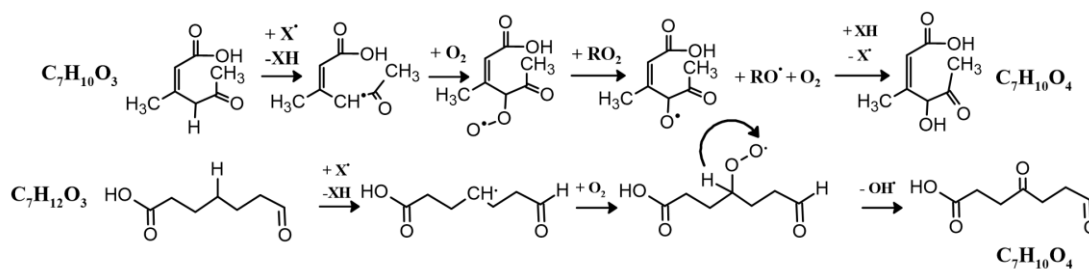
Scheme 7. Formation of 6-oxo-heptanoic acid by the addition of OH to the endo-cyclic double bond of 1M1CHX.

Additionally, the oxidation of the aldehyde group in the $C_7H_{12}O_2$ isomers identified in our samples can be one of the pathways leading to the formation of $C_7H_{12}O_3$ isomers. A similar observation was noted in the MS/MS spectra of $C_7H_8O_3$ and $C_7H_{10}O_4$ isomers, which were detected with weak signals in each MCHX isomer oxidation sample. Due to the poor quality of the chromatograms obtained for these isomers, it was difficult to determine if any were formed in common during the oxidation of the three fuels. $C_7H_8O_3$ isomers are expected to be olefinic KHPs. As for the previously discussed compounds, the MS/MS spectra of the aforementioned isomers show similar fragments, although with varying intensities. The observed fragments suggest the presence of both carboxylic acid and carbonyl groups in their structures, indicating that these compounds may be keto/aldo-carboxylic acids. The oxidation of $C_7H_{10}O_3$ isomers, followed by HO_2 radical elimination, as shown in Scheme 8, can lead to the formation of the family of $C_7H_8O_3$ isomers.



Scheme 8. Formation of aldo-carboxylic acid $C_7H_8O_3$ from the oxidation of KHP $C_7H_{10}O_3$, followed by HO_2 elimination.

Similarly, $C_7H_{10}O_4$ isomers are expected to be olefinic hydroperoxides. Signals corresponding to $C_7H_9D_1O_4$ ($C_7H_{10}D_1O_4^+$, m/z 160.0714) and $C_7H_8D_2O_4$ ($C_7H_9D_2O_4^+$, m/z 161.0777) were detected, confirming the presence of these intermediates. However, DNPH derivatization allows us to distinguish between dihydroperoxides and other isomers containing a $C=O$ group. The MS/MS spectra of these latter suggest the presence of both carboxylic acid and carbonyl groups. The identity of the third oxygenated function could not be determined from the MS/MS spectra; it could be either a carbonyl or hydroxyl group. There are multiple possible formation pathways for $C_7H_{10}O_4$ isomers. One of them could involve the oxidation of $C_7H_{10}O_3$, or possibly from $C_7H_{12}O_3$ isomers, such as 6-oxo-heptanoic acid detected in the 1M1CHX oxidation sample, as illustrated in Scheme 9.



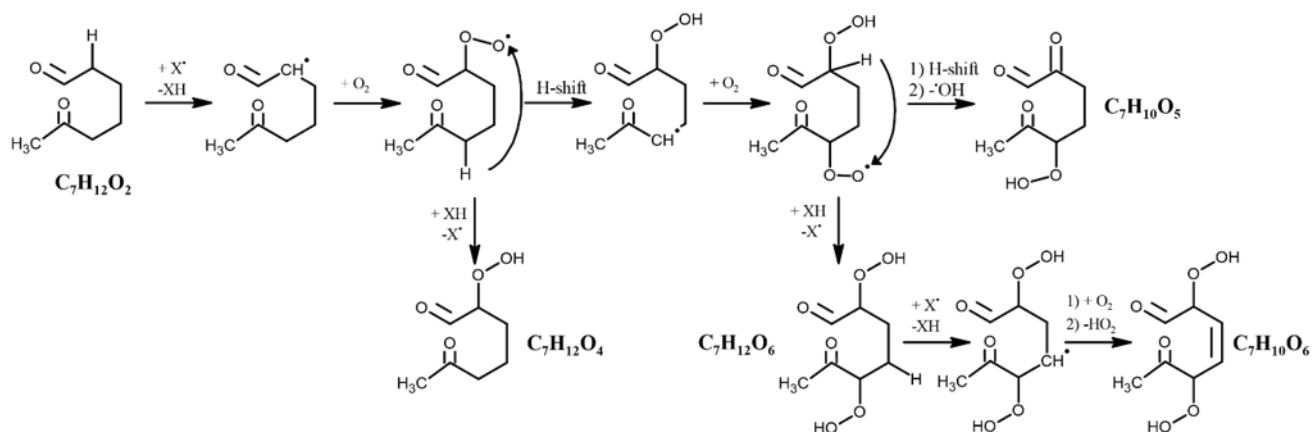
Scheme 9. Possible formation mechanisms for $C_7H_{10}O_4$ isomers.

3.5 Other Oxygenated and Poly-Oxygenated Compounds. After the second O_2 addition to a fuel radical, as shown in Scheme 1, the radical $\cdot OOQOOH$ is formed. An intramolecular H-transfer can then occur. If this transfer happens on the carbon with the OOH group, KHPs are formed following the dissociation of the O-OH bond. However, if the transfer occurs on another carbon atom, the radical can continue to react with O_2 molecules, leading to a third addition of O_2 to the fuel radical $R\cdot$. This results in the formation of the radical $\cdot OOP(OOH)_2$. This sequence of hydrogen shifting and O_2 addition can continue, ultimately leading to the formation of highly oxidized products⁵⁸⁻⁵⁹.

In the oxidation samples of MCHX isomers, and in addition to the oxygenated species previously identified and discussed, other species containing four or more oxygen atoms were also detected. Due to challenges with RP-UHPLC separation and weak ionic signals, FIA-APCI-HRMS was employed for further analyses. Among these species, we detected: $C_7H_8O_4$ ($C_7H_7O_4^-$, m/z 155.0349), $C_7H_8O_5$ ($C_7H_7O_5^-$, m/z 171.0299), $C_7H_{10}O_5$ ($C_7H_9O_5^-$, m/z 173.0455), $C_7H_{10}O_6$ ($C_7H_9O_6^-$, m/z 189.0404), $C_7H_{10}O_7$ ($C_7H_9O_7^-$, m/z 205.0353), and $C_7H_{10}O_9$ ($C_7H_9O_9^-$, m/z 237.00252). Moreover, other poly-oxygenated species with the same number of hydrogen atoms as the fuels were also detected, including: $C_7H_{12}O_4$ ($C_7H_{11}O_4^-$, m/z 159.0662), $C_7H_{12}O_5$ ($C_7H_{11}O_5^-$, m/z 175.0612), $C_7H_{12}O_6$ ($C_7H_{11}O_6^-$, m/z 191.0561), $C_7H_{12}O_7$ ($C_7H_{11}O_7^-$, m/z 207.0510), and $C_7H_{12}O_9$ ($C_7H_{11}O_9^-$, m/z 239.0408).

The determination of the chemical family of these species was not possible. As previously mentioned, weak ion signals were obtained for some species, approaching the detection limit. Consequently, H/D exchange and DNPH derivatization were not observed. Indeed, the efficiency of the reaction with 2,4-DNPH is influenced by the size of the molecule and the number of atoms it contains⁶⁰. In the case of large oxidation products, such as the $C_7H_{10}O_{5,6,7, \text{ or } 9}$ isomers, the reaction with 2,4-DNPH might be limited by steric effects due to the size and complexity of these molecules.

Poly-oxygenated compounds can be formed from radicals other than the initial fuel radicals. For example, oxidation intermediates such as $C_7H_{12}O_2$ isomers detected in the MCHX oxidation samples, including 6-oxo-heptanal found in the 1M1CHX sample, can undergo hydrogen abstraction. This process produces radicals that can subsequently react with O_2 to form poly-oxygenated compounds. An example of this reaction pathway is illustrated in Scheme 10.



Scheme 10. Possible formation mechanisms of poly-oxygenated species.

Furthermore, a wide range of oxidation products with molecular weights from 96 to 240 g/mol were formed during the oxidation of 1M1CHX, 3M1CHX, and 4M1CHX. These products were detected using RP-UHPLC-APCI-HRMS (positive or negative mode) analyses, as shown in Tables S2, S3, and S4, respectively. Among these products, isomers of C_6H_8O , $C_6H_6O_2$, $C_6H_8O_2$, $C_6H_{10}O_2$, $C_6H_{10}O_3$, $C_7H_{12}O$, etc. were observed.

On the other hand, as noted above, many common chemical formulas were detected by HRMS during the oxidation of MCHX hydrocarbons. However, it is important to note that these do not all correspond to the same isomers, as observed for the $C_7H_{10}O_3$ isomers discussed earlier. Nevertheless, they do share similar chemical functionalities. The presence of these products confirms the similarity of the oxidation mechanisms of the MCHX isomers in the JSR and demonstrates that they show comparable kinetics. At the same time, we observed a significant number of common isomers, although their intensities vary from one fuel to another. In other words, these isomers are present in varying amounts. This is the case for $C_7H_{10}O$, $C_7H_{12}O_2$, $C_7H_{12}O_3$, and C_7H_8O (cresol) isomers discussed above. The differences in intensity among these species, likely reflecting their respective quantities, are related to the significance of the reactions during oxidation, possibly influenced by the position of the methyl group in the fuels with respect to the double bond. Finally, the presence of some common isomers may be attributed to isomerization reactions induced by the presence of the endocyclic double bond in the fuels, which stabilizes the radicals formed during the oxidation process through resonance.

4. CONCLUSION

The oxidation of 1M1CHX- O_2 - N_2 , 3M1CHX- O_2 - N_2 , and 4M1CHX- O_2 - N_2 mixtures was carried out in a JSR at 10 bar and for temperatures in the range 500 to 1150 K under fuel-lean conditions ($\phi = 0.5$) with a residence time of 2 s. Under these conditions, GC-FID analyses showed a relatively high fuel conversion (~ 60 - 70 %) in the cool flame regime (<700 K). For the characterization of specific low-temperature oxidation products, samples were collected by bubbling them in cold ACN and were then

analyzed by RP-UHPLC-HRMS and FIA-HRMS. H/D exchange and reactions with 2,4-DNPH were used to confirm the presence of OH or OOH groups and C=O groups, respectively. Additionally, MS/MS analyses at 10 eV enabled the characterization of some oxidation intermediates and the determination of their chemical families through fragment analysis. All these analyses revealed that a large dataset of oxidation products was formed. The oxidation samples of each MCHX isomer contained products resulting from the initial O₂ addition to the fuel radicals, up to and including the fourth addition: C₇H₁₂O₂, C₇H₁₂O₃, C₇H₁₂O₄, C₇H₁₂O₇, C₇H₁₂O₉, C₇H₁₂O₆, C₇H₁₀O, C₇H₁₀O₂, C₇H₁₀O₃, C₇H₁₀O₄, C₇H₁₀O₆, C₇H₁₀O₇, C₇H₁₀O₉, C₇H₈O₂, C₇H₈O₃, C₇H₈O₄, and C₇H₈O₅. Reaction pathways were proposed to explain the formation of oxidation products. These include autoxidation and Korcek mechanism. Moreover, common products for the three hydrocarbons were observed, as well as products from the same chemical family or containing similar chemical functionalities with varying abundances, depending on the hydrocarbon. Whereas multiple reaction pathways can yield the same products or their position isomers, this observation suggests that similar kinetic reaction mechanisms were likely involved in the oxidation of the three tested isomers, leading to the formation of the aforementioned products. Consequently, the three hydrocarbons show comparable kinetic behavior during the studied oxidation process. Only a slight difference in terms of fuel conversion versus temperature between these three isomers was observed. Under the applied conditions, 1M1CHX reacts according to the Waddington mechanism, unlike 3M1CHX and 4M1CHX for which corresponding products could not be detected. However, this mechanism was not significantly important during the oxidation process of 1M1CHX. Our findings are expected to help understanding the oxidation of complex endocyclic alkene-based fuels, such as terpenes, and proposing kinetic reaction mechanisms for their oxidation and that of simpler fuels containing similar chemical structures.

ASSOCIATED CONTENT

Supporting Information

The Supporting Information is available free of charge at <https://pubs.acs.org/doi/>

Fuels properties

Chromatograms before and after reaction with 2,4-DNPH

Chromatograms of oxidation products and standards

Tables of detected formulas in oxidation products by Orbitrap

MS/MS spectra

Structure of ketohydroperoxides deriving from fuels oxidation

Reaction pathways for ketohydroperoxides

AUTHORS INFORMATION

Corresponding Author

Philippe Dagaut – Centre National de la Recherche Scientifique, Institut de Combustion, Aérothermique, Réactivité et Environnement (ICARE), 1C Avenue de la recherche scientifique, 45071 cedex 2, Orléans, France ; orcid.org/0000-0003-4825-3288; Phone: +33 238255466; Email: dagaut@cnsr-orleans.fr

ACKNOWLEDGMENTS

Support from the CAPRYSES project (ANR-11-LABX-006–01) funded by ANR through the PIA (Programme d'Investissement d'Avenir) is gratefully acknowledged. ZD and BH thank the MESRI (French Ministry of Research and Higher Education) for Ph.D. grants.

REFERENCES

- (1) Silvestre, A. J.; Gandini, A., Terpenes: major sources, properties and applications. In *Monomers, polymers and composites from renewable resources*, Elsevier: 2008; pp 17-38.
- (2) Jiang, Z.; Kempinski, C.; Chappell, J., Extraction and Analysis of Terpenes/Terpenoids. *Current Protocols in Plant Biology* **2016**, *1* (2), 345-358.
- (3) Martignago, C. C. S.; Soares-Silva, B.; Parisi, J. R.; Silva, L. C. S. e.; Granito, R. N.; Ribeiro, A. M.; Renno, A. C. M.; de Sousa, L. R. F.; Aguiar, A. C. C., Terpenes extracted from marine sponges with antioxidant activity: a systematic review. *Natural Products and Bioprospecting* **2023**, *13* (1), 23.
- (4) Salha, G. B.; Abderrabba, M.; Labidi, J., A status review of terpenes and their separation methods. *Reviews in Chemical Engineering* **2021**, *37* (3), 433-447.
- (5) González-Hernández, R. A.; Valdez-Cruz, N. A.; Trujillo-Roldán, M. A., Factors that influence the extraction methods of terpenes from natural sources. *Chem. Pap.* **2024**, *78* (5), 2783-2810.
- (6) Cox-Georgian, D.; Ramadoss, N.; Dona, C.; Basu, C., Therapeutic and Medicinal Uses of Terpenes. In *Medicinal Plants: From Farm to Pharmacy*, Joshee, N.; Dhekney, S. A.; Parajuli, P., Eds. Springer International Publishing: Cham, 2019; pp 333-359.
- (7) Del Prado-Audelo, M. L.; Cortés, H.; Caballero-Florán, I. H.; González-Torres, M.; Escutia-Guadarrama, L.; Bernal-Chávez, S. A.; Giraldo-Gomez, D. M.; Magaña, J. J.; Leyva-Gómez, G., Therapeutic Applications of Terpenes on Inflammatory Diseases. *Frontiers in Pharmacology* **2021**, *12*, 704197.
- (8) Fan, M.; Yuan, S.; Li, L.; Zheng, J.; Zhao, D.; Wang, C.; Wang, H.; Liu, X.; Liu, J., Application of Terpenoid Compounds in Food and Pharmaceutical Products. *Fermentation* **2023**, *9* (2), 119.
- (9) Volcho, K.; Anikeev, V., Chapter 3 - Environmentally Benign Transformations of Monoterpenes and Monoterpenoids in Supercritical Fluids. 2014; pp 69-87.
- (10) Ninkuu, V.; Zhang, L.; Yan, J.; Fu, Z.; Yang, T.; Zeng, H., Biochemistry of Terpenes and Recent Advances in Plant Protection. *Int J Mol Sci* **2021**, *22* (11) 5710.
- (11) Paulino, B. N.; Silva, G. N. S.; Araújo, F. F.; Néri-Numa, I. A.; Pastore, G. M.; Bicas, J. L.; Molina, G., Beyond natural aromas: The bioactive and technological potential of monoterpenes. *Trends in Food Science & Technology* **2022**, *128*, 188-201.

- (12) Filley, J.; Miedaner, A.; Ibrahim, M.; Nimlos, M. R.; Blake, D. M., Energetics of the 2+2 cyclization of limonene. *Journal of Photochemistry and Photobiology A: Chemistry* **2001**, *139* (1), 17-21.
- (13) Pahima, E.; Hoz, S.; Ben-Tzion, M.; Major, D. T., Computational design of biofuels from terpenes and terpenoids. *Sustainable Energy & Fuels* **2019**, *3* (2), 457-466.
- (14) Peralta-Yahya, P. P.; Ouellet, M.; Chan, R.; Mukhopadhyay, A.; Keasling, J. D.; Lee, T. S., Identification and microbial production of a terpene-based advanced biofuel. *Nature Communications* **2011**, *2* (1), 483.
- (15) Peralta-Yahya, P. P.; Zhang, F.; del Cardayre, S. B.; Keasling, J. D., Microbial engineering for the production of advanced biofuels. *Nature* **2012**, *488* (7411), 320-8.
- (16) Mewalal, R.; Rai, D. K.; Kainer, D.; Chen, F.; Külheim, C.; Peter, G. F.; Tuskan, G. A., Plant-Derived Terpenes: A Feedstock for Specialty Biofuels. *Trends Biotechnol* **2017**, *35* (3), 227-240.
- (17) Harvey, B. G.; Wright, M. E.; Quintana, R. L., High-Density Renewable Fuels Based on the Selective Dimerization of Pinenes. *Energy Fuels* **2010**, *24* (1), 267-273.
- (18) Meylemans, H. A.; Quintana, R. L.; Harvey, B. G., Efficient conversion of pure and mixed terpene feedstocks to high density fuels. *Fuel* **2012**, *97*, 560-568.
- (19) Lapuerta, M.; Tobío-Pérez, I.; Ortiz-Alvarez, M.; Donoso, D.; Canoira, L.; Piloto-Rodríguez, R., Heterogeneous Catalytic Conversion of Terpenes into Biofuels: An Open Pathway to Sustainable Fuels. *Energies* **2023**, *16* (6), 2526.
- (20) Micheli, L.; Módolo, D.; Pereira, L., Effects of the use of D-limonene as an additive to diesel-biodiesel blends on exhaust gases composition of compression ignition engines. *Revista de Engenharia Térmica* **2018**, *17*, 33.
- (21) Mack, J. H.; Rapp, V. H.; Broeckelmann, M.; Lee, T. S.; Dibble, R. W., Investigation of biofuels from microorganism metabolism for use as anti-knock additives. *Fuel* **2014**, *117*, 939-943.
- (22) Lee, S. K.; Chou, H.; Ham, T. S.; Lee, T. S.; Keasling, J. D., Metabolic engineering of microorganisms for biofuels production: from bugs to synthetic biology to fuels. *Curr Opin Biotechnol* **2008**, *19* (6), 556-63.
- (23) Beller, H. R.; Lee, T. S.; Katz, L., Natural products as biofuels and bio-based chemicals: fatty acids and isoprenoids. *Natural Product Reports* **2015**, *32* (10), 1508-1526.
- (24) Bergman, A.; Siewers, V., Chapter 7 - Metabolic Engineering Strategies to Convert Carbohydrates to Aviation Range Hydrocarbons. In *Biofuels for Aviation*, Chuck, C. J., Ed. Academic Press: 2016; pp 151-190.
- (25) Woodroffe, J.-D.; Harvey, B. G., High-Performance, Biobased, Jet Fuel Blends Containing Hydrogenated Monoterpenes and Synthetic Paraffinic Kerosenes. *Energy Fuels* **2020**, *34* (5), 5929-5937.
- (26) Dbouk, Z.; Belhadj, N.; Lailliau, M.; Benoit, R.; Dagaut, P., Characterization of the Autoxidation of Terpenes at Elevated Temperature Using High-Resolution Mass Spectrometry: Formation of Ketohydroperoxides and Highly Oxidized Products from Limonene. *Journal of Physical Chemistry A* **2022**, *126* (48), 9087-9096.
- (27) Dbouk, Z.; Belhadj, N.; Lailliau, M.; Benoit, R.; Dagaut, P., On the autoxidation of terpenes: Detection of oxygenated and aromatic products. *Fuel* **2024**, *358*, 130306.
- (28) Ranzi, E.; Cavallotti, C.; Cuoci, A.; Frassoldati, A.; Pelucchi, M.; Faravelli, T., New reaction classes in the kinetic modeling of low temperature oxidation of n-alkanes. *Combustion and Flame* **2015**, *162* (5), 1679-1691.
- (29) Liu, B.; Di, Q.; Lailliau, M.; Belhadj, N.; Dagaut, P.; Wang, Z., Experimental and kinetic modeling study of low-temperature oxidation of n-pentane. *Combustion and Flame* **2023**, *254*, 112813.
- (30) Wang, Z.; Hansen, N.; Jasper, A. W.; Chen, B.; Popolan-Vaida, D. M.; Yalamanchi, K. K.; Najjar, A.; Dagaut, P.; Sarathy, S. M., Cool flame chemistry of diesel surrogate compounds: n-Decane, 2-methylnonane, 2,7-dimethyloctane, and n-butylcyclohexane. *Combustion and Flame* **2020**, *219*, 384-392.
- (31) Popolan-Vaida, D. M.; Eskola, A. J.; Rotavera, B.; Lockyear, J. F.; Wang, Z.; Sarathy, S. M.; Caravan, R. L.; Zádor, J.; Sheps, L.; Lucassen, A., et al., Formation of Organic Acids and Carbonyl Compounds in n-Butane Oxidation via γ -Ketohydroperoxide Decomposition. *Angewandte Chemie International Edition* **2022**, *61* (42), e202209168.

- (32) Xie, C.; Lailliau, M.; Issayev, G.; Xu, Q.; Chen, W.; Dagaut, P.; Farooq, A.; Sarathy, S. M.; Wei, L.; Wang, Z., Revisiting low temperature oxidation chemistry of n-heptane. *Combust. Flame* **2022**, *242*, 112177.
- (33) Belhadj, N.; Benoit, R.; Dagaut, P.; Lailliau, M.; Serinyel, Z.; Dayma, G., Oxidation of di-n-propyl ether: Characterization of low-temperature products. *Proc. Combust. Inst.* **2021**, *38* (1), 337-344.
- (34) Li, Y.; Zhao, Q.; Zhang, Y.; Huang, Z.; Sarathy, S. M., A Systematic Theoretical Kinetics Analysis for the Waddington Mechanism in the Low-Temperature Oxidation of Butene and Butanol Isomers. *The Journal of Physical Chemistry A* **2020**, *124* (27), 5646-5656.
- (35) Berndt, T.; Richters, S.; Kaethner, R.; Voigtländer, J.; Stratmann, F.; Sipilä, M.; Kulmala, M.; Herrmann, H., Gas-phase ozonolysis of cycloalkenes: formation of highly oxidized RO₂ radicals and their reactions with NO, NO₂, SO₂, and other RO₂ radicals. *The Journal of Physical Chemistry A* **2015**, *119* (41), 10336-10348.
- (36) Rissanen, M. P.; Kurten, T.; Sipilä, M.; Thornton, J. A.; Kausiala, O.; Garmash, O.; Kjaergaard, H. G.; Petaja, T.; Worsnop, D. R.; Ehn, M., Effects of chemical complexity on the autoxidation mechanisms of endocyclic alkene ozonolysis products: From methylcyclohexenes toward understanding alpha-pinene. *J. Phys. Chem. A* **2015**, *119*, 4633.
- (37) Hatakeyama, S.; Akimoto, H., Reactions of Ozone with 1-Methylcyclohexene and Methylene-cyclohexane in Air. *Bulletin of the Chemical Society of Japan* **2006**, *63* (9), 2701-2703.
- (38) Keywood, M. D.; Varutbangkul, V.; Bahreini, R.; Flagan, R. C.; Seinfeld, J. H., Secondary organic aerosol formation from the ozonolysis of cycloalkenes and related compounds. *Environ Sci Technol* **2004**, *38* (15), 4157-64.
- (39) Gao, S.; Keywood, M.; Ng, N. L.; Surratt, J.; Varutbangkul, V.; Bahreini, R.; Flagan, R. C.; Seinfeld, J. H., Low-Molecular-Weight and Oligomeric Components in Secondary Organic Aerosol from the Ozonolysis of Cycloalkenes and α -Pinene. *The Journal of Physical Chemistry A* **2004**, *108* (46), 10147-10164.
- (40) Liang, J. H.; Cao, S. T.; Li, F.; Li, X. L.; He, R. N.; Bai, X.; Wang, Q. D.; Li, Y., A comparative single-pulse shock tube experiment and kinetic modeling study on pyrolysis of cyclohexane, methylcyclohexane and ethylcyclohexane. *Defence Technology* **2023**, *20*, 137-148.
- (41) Zhang, F.; Wang, Z.; Wang, Z.; Zhang, L.; Li, Y.; Qi, F., Kinetics of Decomposition and Isomerization of Methylcyclohexane: Starting Point for Studying Monoalkylated Cyclohexanes Combustion. *Energy Fuels* **2013**, *27* (3), 1679-1687.
- (42) Dagaut, P.; Reuillon, M.; Cathonnet, M., Experimental-Study of the Oxidation of N-Heptane in a Jet-Stirred Reactor from Low-Temperature to High-Temperature and Pressures up to 40-Atm. *Combust. Flame* **1995**, *101* (1-2), 132-140.
- (43) Ranzi, E.; Gaffuri, P.; Faravelli, T.; Dagaut, P., A Wide-Range Modeling Study of N-Heptane Oxidation. *Combust. Flame* **1995**, *103* (1-2), 91-106.
- (44) Dagaut, P.; Cathonnet, M.; Rouan, J. P.; Foulatier, R.; Quilgars, A.; Boettner, J. C.; Gaillard, F.; James, H., A jet-stirred reactor for kinetic studies of homogeneous gas-phase reactions at pressures up to ten atmospheres (≈ 1 MPa). *Journal of Physics E: Scientific Instruments* **1986**, *19* (3), 207.
- (45) Dagaut, P.; Cathonnet, M.; Boettner, J. C., Experimental study and kinetic modeling of propene oxidation in a jet stirred flow reactor. *The Journal of Physical Chemistry* **1988**, *92* (3), 661-671.
- (46) Chakir, A.; Bellimam, M.; Boettner, J. C.; Cathonnet, M., Kinetic Study of N-Pentane Oxidation. *Combust. Sci. Technol.* **1991**, *77* (4-6), 239-260.
- (47) Dayma, G.; Hadj Ali, K.; Dagaut, P., Experimental and detailed kinetic modeling study of the high pressure oxidation of methanol sensitized by nitric oxide and nitrogen dioxide. *Proc. Combust. Inst.* **2007**, *31* (1), 411-418.
- (48) Benoit, R.; Belhadj, N.; Dbouk, Z.; Lailliau, M.; Dagaut, P., On the formation of highly oxidized pollutants by autoxidation of terpenes under low-temperature-combustion conditions: the case of limonene and α -pinene. *Atmospheric Chemistry and Physics* **2023**, *23* (10), 5715-5733.
- (49) Herbinet, O.; Husson, B.; Ferrari, M.; Glaude, P.-A.; Battin-Leclerc, F., Low temperature oxidation of benzene and toluene in mixture with n-decane. *Proceedings of the Combustion Institute* **2013**, *34* (1), 297-305.

- (50) Schwantes, R. H.; Schilling, K. A.; McVay, R. C.; Lignell, H.; Coggon, M. M.; Zhang, X.; Wennberg, P. O.; Seinfeld, J. H., Formation of highly oxygenated low-volatility products from cresol oxidation. *Atmos. Chem. Phys.* **2017**, *17* (5), 3453-3474.
- (51) Liang, Y.; Simón-Manso, Y.; Neta, P.; Stein, S. E., Unexpected Gas-Phase Nitrogen–Oxygen Smiles Rearrangement: Collision-Induced Dissociation of Deprotonated 2-(N-Methylanilino)ethanol and Morpholinylbenzoic Acid Derivatives. *J. Am. Soc. Mass Spectrom.* **2022**, *33* (11), 2120-2128.
- (52) Demarque, D. P.; Crotti, A. E. M.; Vessecchi, R.; Lopes, J. L. C.; Lopes, N. P., Fragmentation reactions using electrospray ionization mass spectrometry: an important tool for the structural elucidation and characterization of synthetic and natural products. *Nat. Prod. Rep.* **2016**, *33* (3), 432-455.
- (53) Goldsmith, C. F.; Green, W. H.; Klippenstein, S. J., Role of O₂ + QOOH in Low-Temperature Ignition of Propane. 1. Temperature and Pressure Dependent Rate Coefficients. *The Journal of Physical Chemistry A* **2012**, *116* (13), 3325-3346.
- (54) Jalan, A.; Alecu, I. M.; Meana-Pañeda, R.; Aguilera-Iparraguirre, J.; Yang, K. R.; Merchant, S. S.; Truhlar, D. G.; Green, W. H., New Pathways for Formation of Acids and Carbonyl Products in Low-Temperature Oxidation: The Korcek Decomposition of γ -Ketohydroperoxides. *Journal of the American Chemical Society* **2013**, *135* (30), 11100-11114.
- (55) Battin-Leclerc, F.; Konnov, A. A.; Jaffrezo, J. L.; Legrand, M., To Better Understand the Formation of Short-Chain Acids in Combustion Systems. *Combustion Science and Technology* **2007**, *180* (2), 343-370.
- (56) Herbinet, O.; Husson, B.; Serinyel, Z.; Cord, M.; Warth, V.; Fournet, R.; Glaude, P. A.; Sirjean, B.; Battin-Leclerc, F.; Wang, Z., et al., Experimental and modeling investigation of the low-temperature oxidation of n-heptane. *Combust Flame* **2012**, *159* (12), 3455-3471.
- (57) Madronich, S.; Chatfield, R. B.; Calvert, J. G.; Moortgat, G. K.; Veyret, B.; Lesclaux, R., A photochemical origin of acetic acid in the troposphere. *Geophys. Res. Lett.* **1990**, *17* (13), 2361-2364.
- (58) Belhadj, N.; Benoit, R.; Dagaut, P.; Lailliau, M., Experimental characterization of n-heptane low-temperature oxidation products including keto-hydroperoxides and highly oxygenated organic molecules (HOMs). *Combust. Flame* **2021**, *224*, 83-93.
- (59) Belhadj, N.; Benoit, R.; Dagaut, P.; Lailliau, M., Experimental Characterization of Tetrahydrofuran Low-Temperature Oxidation Products Including Ketohydroperoxides and Highly Oxygenated Molecules. *Energy Fuels* **2021**, *35* (9), 7242–7252.
- (60) Uchiyama, S.; Inaba, Y.; Kunugita, N., Derivatization of carbonyl compounds with 2, 4-dinitrophenylhydrazine and their subsequent determination by high-performance liquid chromatography. *Journal of Chromatography B* **2011**, *879* (17-18), 1282-1289.

TOC Graphic

